Repairing human tooth enamel with leucine-rich amelogenin peptide–chitosan hydrogel

Kaushik Mukherjee, Qichao Ruan, and David Liberman
Center for Craniofacial Molecular Biology, Division of Biomedical Sciences, Herman Ostrow School of Dentistry, University of Southern California, Los Angeles, California 90033, USA

Shane N. White
Section of Endodontics, Constitutive & Regenerative Sciences, School of Dentistry, University of California, Los Angeles, California 90095, USA

Janet Moradian-Oldak[a)]
Center for Craniofacial Molecular Biology, Division of Biomedical Sciences, Herman Ostrow School of Dentistry, University of Southern California, Los Angeles, California 90033, USA

(Received 14 July 2015; accepted 30 January 2016)

We have recently reported the repair of carious enamel using a full-length amelogenin–chitosan hydrogel through guided stabilization and growth of mineral clusters. The objective of this study was to further evaluate the enamel repair potential of smaller amelogenin peptides like LRAP (leucine-rich amelogenin peptide) and compare their efficiency with their full-length counterpart. The demineralized tooth slices treated with a single application of LRAP–chitosan hydrogel for 3 days showed a dense mineralized layer consisting of highly organized enamel-like apatite crystals. Focus-ion beam technique showed a seamless growth at the interface between the repaired layer and native enamel. There was a marked improvement in the surface hardness after treatment of the demineralized sample with almost 87% recovery of the hardness value to that of sound enamel sections. This current approach can inspire the design of smaller peptide analogues based on naturally occurring amelogenin as a competent, low-cost, and safe strategy for enamel biomimetics to curb the high prevalence of incipient dental caries.

I. INTRODUCTION

Vertebrate dental enamel is a supreme case of biomineralization, being composed of about 97% carbonated hydroxyapatite by weight, providing masticatory function for a lifetime and lasting for millennia, unless attacked by caries.[1,2] The inorganic content of enamel has a highly organized microarchitecture that is made up of fundamental organizational units called enamel rods (prisms) and inter-rods interwoven in densely packed arrays of hydroxyapatite crystals.[3] Enamel formation or amelogenesis takes place in a highly regulated environment mediated by organic matrices rich in matrix proteins, primarily amelogenin, which constitutes almost 90% of the organic content.[4] Protein–protein, protein–mineral and protein–protease interactions orchestrate the formation, growth, and alignment of the crystallites to form a highly intricate prism pattern.[5] This hierarchical arrangement within the enamel is an important factor in imparting the robust mechanical properties to the tissue for protection against cariogenic bacteria and mechanical force during tooth functioning. Interestingly, unlike other mineralized tissues such as dentin or bone, enamel is acellular in nature and therefore cannot regenerate or actively repair itself. This unique restriction makes enamel an interesting target for future biomimetic and therapeutic approaches in dentistry. However, it is now known that crystallite orientation is preserved throughout, even in moderate carious lesions, which facilitate the identification of preventive remineralizing strategies with the potential to recreate the original nanostructure.[6]

Currently, the restorative materials used for the treatment of enamel defects in clinical practice include resin-composite, cements, ceramics, and amalgam. However, these materials lack the composition, chemical properties, graded anisotropy, and structural framework of enamel crystals which compromises their bonding strength at the tooth interface, leading to incidences of marginal leakage, secondary caries, and eventually failure of the restoration. Hence, designing innovative means of replicating enamel-like tissue is needed to advance dental material science. Several strategies have been proposed to replicate the enamel microstructure using chemicals,

Contributing Editor: Michelle L. Oyen
[a)]Address all correspondence to this author.
e-mail: joldak@usc.edu
DOI: 10.1557/jmr.2016.64

 © Materials Research Society 2016

https://doi.org/10.1557/jmr.2016.64 Published online by Cambridge University Press

polymers, amorphous calcium phosphate (ACP) nanoparticles, dendrimers, and hydrogels.[7] New approaches to enamel remineralization have included the use of β-sheet forming peptides,[8] electrospun mats of ACP/poly (vinylpyrrolidone) nanofibers,[9] amelogenin-releasing system,[10] and casein phosphopeptide stabilized ACP.[11] Yamagishi et al. have developed a dental paste that upon application on the enamel surface, under acidic pH, resulted in the formation of organized nanocrystals of apatite.[12] However, the native enamel structure is a highly complex tissue that is extremely difficult to recapitulate within a relatively short period of time. Recently, we developed an amelogenin (rP172)–chitosan hydrogel as a novel biomimetic material to promote the regrowth of enamel crystals on acid-etched lesions and observed a robust interface between the newly formed layer and native enamel.[13,14]

To improve the clinical feasibility of this protein–gel system, we incorporated a smaller, cost-effective amelogenin-derived peptide to the chitosan hydrogel that could (a) regulate biomimetic enamel regrowth on a carious model and (b) act as an effective substitute for our previously synthesized full-length amelogenin–chitosan hydrogel with potential applications in enamel repair.

Leucine-rich amelogenin peptide (LRAP) was used as a promising substitute for the full-length amelogenin in mediating organized crystal growth. LRAP is a 58-residue alternatively spliced mRNA transcript of full-length amelogenin and a product of exons 2, 3, 5, and the end of exons 6 and 7.[15] It conserves the end terminals of the native protein, specifically the hydrophilic residues of the C- and inner N-termini that interact with HAP to direct mineral growth and for mineral binding.[16,17] Since interaction of the charged residues with the crystal surface plays a vital role in the biomineralization process,[18–20] LRAP proves to be an excellent model substitute for the full-length amelogenin in eliciting details about the secondary structure and orientation of the peptide at the apatite interface.[16,21,22] Although previous studies suggested that LRAP is a HAP crystal growth inhibitor,[15] current studies indicate that it may have an important function in promoting enamel mineralization.[23,24] Several other functions have also been attributed to LRAP in vivo, including that of a cell-signaling molecule capable of inducing osteogenesis in different cell types such as mouse cementoblasts[25] and embryonic stem cells.[26]

In this in vitro study, phosphorylated human LRAP was added to a chitosan hydrogel (LRAP–CS) to determine whether it could promote aligned crystal growth for biomimetic repair as effectively as the full-length amelogenin (rP172) in minimal treatment time. After the remineralization cycle, the microstructure, composition, orientation, and hardness value (HV) of the regrown crystals were investigated by scanning electron microscopy (SEM), X-ray diffraction (XRD), focus-ion beam (FIB), transmission electron microscopy (TEM), and Vickers microhardness (VMH) test. We demonstrate the growth of organized de novo aprismatic crystals on demineralized enamel surfaces in the presence of LRAP–chitosan hydrogel that showed significant hardness of the demineralized enamel surface, after only 3 days of treatment. Our study further elucidates the possible role of this peptide in the biomineralization events occurring in enamel.

II. EXPERIMENT

A. Preparation of LRAP

Human LRAP was synthesized by Chempeptide Limited (Shanghai, China). The peptide was phosphorylated at Ser-16 as shown in Fig. 1. HPLC (high performance liquid chromatography) and mass spectrometry were used for peptide purification and determination. The peptide (more than 95% purity) was weighed and dissolved in distilled water to yield a stock solution of 2 mg/ml and centrifuged (8000 rpm, 1 min). The stock solution was placed in a slow shaker for 4 h and divided into aliquots of 100 μL/tube. The aliquots were then lyophilized for 12 h and the final concentration of peptide used was 200 μg per tube.

B. Tooth slice preparation and artificial demineralization

Sound human third molars (extracted under the standard procedures for extraction at the Ostrow School of Dentistry of the University of Southern California and handled with the approval of the Institutional Review Board) were sectioned longitudinally into 1 mm thick slices using a water-cooled slow speed diamond saw. The slices were polished using a fine grid paper and then sonicated in a water bath for 2 min. The surfaces of the samples were partly painted with a layer of acid-resistant nail varnish, leaving only an exposed window of dimensions 3 × 2 mm^2. The tooth samples were dried for 2 h after varnish application. The slices were then exposed to a demineralization buffer (1.5 mM $CaCl_2{\cdot}2H_2O$, 0.9 mM KH_2PO_4, 50 mM sodium acetate, 300 ppm NaF) at pH 4.6 for 7 days at room temperature (RT), rinsed, and dried.

C. Repair of demineralized enamel using the LRAP–chitosan hydrogel

The LRAP–containing chitosan (medium molecular weight, 75–85% deacetylated, Sigma-Aldrich, St. Louis, Missouri) hydrogel was prepared using the protocol developed by Ruan et al., 2013. One mL of chitosan calcium phosphate solution (960 μL of 2% chitosan + 25 μL of 0.1 M $CalCl_2$ and 15 μL of 0.1 M Na_2HPO_4) was mixed with LRAP (200 μg), followed by stirring at room temperature overnight. NaOH (1 M) was added to the hydrogel to bring the pH to a final value of 6.5. The treatment consisted of a 20 μL application to each window (using a BD 1 mL syringe for the hydrogel; Becton,

https://doi.org/10.1557/jmr.2016.64 Published online by Cambridge University Press

Human LRAP (+P):

MPLPPHPGHPGYINF***pS***YEVLTPLKWYQSIRPPPLPPMLPDLTLEAWPSTDKTKREEVD

FIG. 1. Amino acid sequence of phosphorylated human LRAP (58-residue). The serine residue in bold is phosphorylated.

Dickinson & Company, East Rutherford, New Jersey) on days 1, 3, and 7, followed by drying in the desiccator for 10 min at RT. The tooth slices were immersed in 5 mL of artificial saliva (1.5 mM $CaCl_2{\cdot}2H_2O$, 20 mM HEPES buffer, 0.9 mM KH_2PO_4, 130 mM KCl, 2.7 ppm F^-, pH 7.0, adjusted with 1 M NaOH) at 37 °C for 3, 7, and 14 days, respectively. The artificial saliva was replenished every 24 h. After incubation, the tooth slices were sonicated in a water bath for 10 min, rinsed with deionized water and air-dried before examination under XRD and SEM.

D. Analysis and imaging of the in situ regrown crystals on tooth enamel

1. Scanning electron microscopy

FESEM (field emission SEM; JEOL JSM-7001F, JEOL Ltd., Tokyo, Japan) imaging was used to explore the tooth slice surfaces for structural analysis after in vitro regrowth experiments. The tooth surfaces were sputtered with Au and observed under an accelerating voltage of 10 kV. Both top-down and side views of the sectioned tooth samples were observed under SEM after biomineralization. To observe the cross section of the regenerated crystal layer, the tooth samples were sectioned in the center of the window to expose the long axis of the enamel prisms. First, a narrow groove was created on the opposite (nonremineralized) side of the tooth surface using a slow speed diamond saw. Then it was snapped into 2 pieces to expose the newly grown layer.

2. X-ray diffraction

X-ray diffraction (XRD; Rigaku diffractometer, Rigaku Corporation, Tokyo, Japan) with Cu K_α radiation (k = 1.542 Å) operating at 70 kV and 50 mA with a sampling step of 0.08 and 2θ of range 5–65° was used to analyze the crystal orientation and mineral phase of the new crystals.

3. FIB-TEM

Thin sections (<100 nm) between enamel and the newly grown layer (3-day sample) for the TEM observations were prepared in a SEM/FIB (JEOL JIB-4500) with an ion accelerating voltage of 30 kV. The device was also equipped with an in situ lift-out system (Omniprobe Autoprobe 200, Oxford Instruments, Vacaville, California), which had a tungsten needle attached to a micromanipulator inside the FIB vacuum chamber. Care was taken to ensure that the lift-out trenches were made on enamel slices with robust newly formed crystals that would correctly represent the interface between the newly formed layer and native enamel when viewed under TEM (JEOL TEM-2100F, JEOL Ltd.). High-resolution transmission electron microscopy (HR-TEM) images were obtained to determine the crystallographic plane and observe the boundary between the newly regrown crystal layer and the native enamel crystal.

E. Surface microhardness of the reconstructed enamel biomimetic layer repaired by using LRAP–CS hydrogel

The microindentation technique was used to record the hardness of sound enamel, demineralized enamel, and newly grown biomimetic layers using a customized manually operated VMH Tester. The samples consisted of tooth sections that were repaired by (a) chitosan only, (b) chitosan–LRAP, and (c) chitosan-full-length amelogenin hydrogel after being immersed in artificial saliva for 3 days (n = 3 for each group). Ten indentations were made in each specimen using a 100 g load force with a 20 s dwell time. One-way ANOVA (analysis of variance) was used to determine if the control and test groups differed with respect to hardness ($P < 0.05$). In the event that groups differed, a Tukey multiple comparison test would be used to identify differences ($P < 0.05$).

III. RESULTS AND DISCUSSION

A. Regrowth of a biomimetic layer on demineralized enamel using LRAP–CS hydrogel

Dental caries occurs as a direct result of destruction/demineralization of the tooth's calcified tissues by acid generated in oral "plaque biofilms".[27] To simulate the acidic oral environment, the tooth slices were immersed in a demineralization solution for 7 days at pH 4.6. The surface topology of the demineralized enamel sections and the control groups after 3 days of regrowth is shown in Fig. 2. Tooth slices treated with chitosan only (used as a negative control) had a very thin and uneven coating of interspersed smaller crystallites ranging from random to well-organized crystals at the end of the remineralization cycle [Fig. 2(b)]. On slices treated with the full-length amelogenin-chitosan hydrogel (used as a positive control), a more uniform layer of well-oriented crystals was observed [Fig. 2(c)]. This was consistent with our previous studies where we compared samples treated by artificial saliva (used as a negative control), chitosan only, and full-length AMEL–CS to evaluate differences in the thickness and crystal orientation of the new crystal

https://doi.org/10.1557/jmr.2016.64 Published online by Cambridge University Press

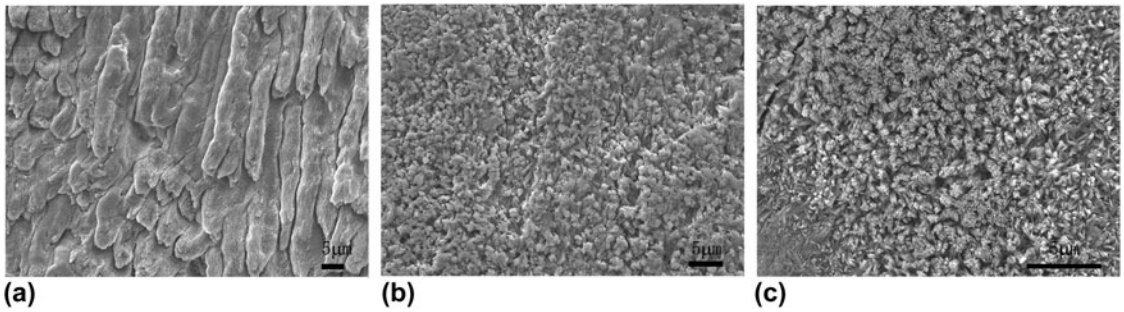


FIG. 2. SEM images of (a) 7-day demineralized enamel and (b and c) newly grown layer treated with the two control groups in artificial saliva for 3 days; (b) chitosan only and (c) AMEL–CS.

layer.[13] Sectioned enamel slices placed in artificial saliva solution for 7 days without application of any hydrogel formed a porous calcium phosphate layer of only ~1 μm thickness on the surface. These crystals were extremely small, unstructured, and bore no resemblance to the native enamel structure.

We observed the regrowth of crystals after 3, 7, and 14 days of treatment with LRAP–CS hydrogel to detect any variations in crystal organization and growth pattern [Figs. 3(a)–3(d)]. While organized layers of apatite crystals were formed in all cases, we focused our attention on the 3-day treated samples to determine whether minimal duration of treatment could promote hardness restoration just as effectively (while comparing it to our controls). Thickness of the newly grown layer did not change with increased mineralization time, neither with the repeated number of hydrogel applications (Fig. S1). However, both increased mineralization time (from 3 to 14 days) as well as the number of hydrogel application drastically increased the extent of mineralization. Much larger area of the remineralized enamel surface was uniformly covered with densely formed apatite crystals. SEM images (top-down view) of the newly grown layers formed after CS and AMEL–CS treatment for 3 days, 7 days, and 14 days are provided in the supplementary material (Fig. S2). After the LRAP–CS hydrogel-coated tooth samples were soaked in artificial saliva for 3 days, SEM was used to observe the morphology and arrangement of the newly grown crystals. The bulk of the native enamel substrate was covered by fine, needle-like, well-organized, closely stacked apatitic crystals similar to what was observed using the full-length amelogenin–chitosan hydrogel (rP172)[13] [Fig. 3(a)]. The new layer formed on the demineralized enamel surface had a thickness of approximately 10 μm [Fig. 3(b)]. It was noted that the regrown crystals differed in their morphology, distribution, and rate of growth over demineralized enamel with LRAP–CS promoting much faster crystal nucleation and growth compared to the control and rP172–CS at the end of the 3-day remineralization cycle. The untreated tooth samples immersed in saliva without application of any hydrogel showed little to no crystal growth due to the absence of an organic mediator that could sequester the mineral ions to form crystals.[13] To view the cross-sectional thickness of the regrown mineral layer, the treated tooth slices soaked in artificial saliva for 3 days were cut longitudinally and observed under SEM [Fig. 3(b)]. The study showed a well-defined assembly of dense apatitic-rods organized parallel to each other along their *c*-axial direction and perpendicular to the original enamel surface. Remarkably, even after sonication for 10 min, the regrown layer remained stable and maintained its thickness. This finding has a clinical significance when durability of dental restoration is concerned. The regulatory effect of LRAP on crystal growth and morphology was found to operate in a time-dependent manner. At the end of 1 week, the crystals remained relatively uniform in size but fused in parts and increased in density, forming a densely packed layer of rod-like crystals [Fig. 3(c)]. However, at the end of 14 days of regrowth, bundles of large, fused crystals arranged in a 'dumb-bell' fashion were observed tightly bound to the enamel slices [Fig. 3(d)]. This unique crystal morphology has been previously observed in the crystallization of minerals and may be attributed to several factors like pH, supersaturation and the presence of charges additives.[28,29] It was not visible in any of the control samples treated with chitosan only or AMEL–CS and may indicate the functionality of charged peptides like LRAP on apatitic surfaces and needs to be investigated further (Fig. S2). The orientation of the newly formed crystals was further established by XRD (Fig. 4). XRD results showed sharp diffraction peaks at $2\theta = 25.8°$ (002), $2\theta = 31.6°$ (211) and $2\theta = 32.1°$ (300) that matched well with the expected peaks for hydroxyapatite (JCPDS 09-0432) and indicated good crystallinity of the layer regrown in LRAP–CS hydrogel. The ratio of the XRD peak intensity (I_{002}:I_{211}) at $2\theta = 25.8°$ to that at $2\theta = 31.6°$ was measured for the different samples to calculate the alignment and specific orientation of the new crystals. The ratios of I_{002}:I_{211} after 3, 7, and 14 days of remineralization using LRAP–CS hydrogel were 0.33, 1.47, and 1.46, respectively. This indicated a gradual improvement in the crystal orientation from

https://doi.org/10.1557/jmr.2016.64 Published online by Cambridge University Press

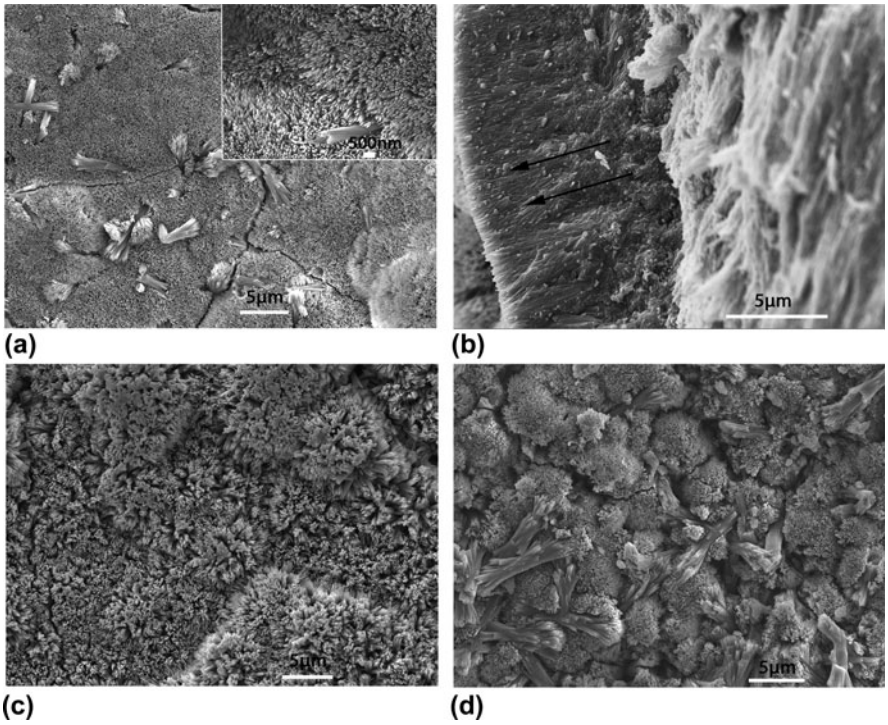


FIG. 3. SEM images of the newly grown layer after remineralization in LRAP–CS hydrogel for (a and b) 3 days (top view and cross-sectional view), (c) 7 days, and (d) 14 days. Hydrogel application was made on days 1, 3, and 7 of 14 days in artificial saliva.

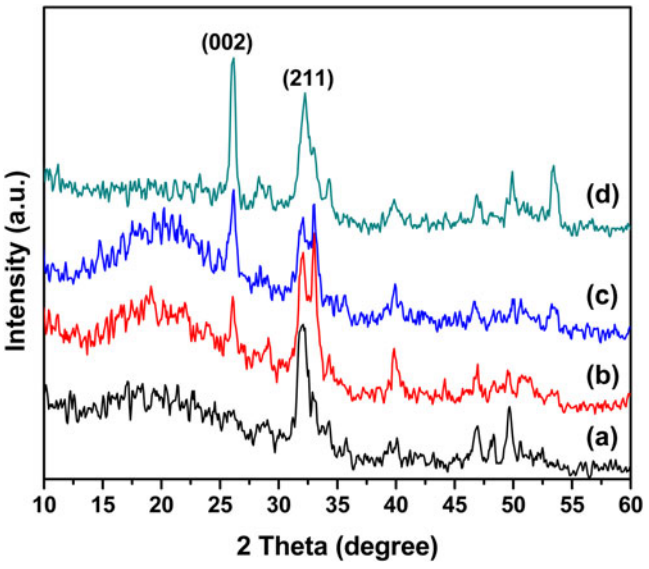


FIG. 4. XRD spectrum of the biomimetic coating on (a) demineralized enamel after being treated with LRAP–CS in artificial saliva for (b) 3 days, (c) 7 days, and (d) 14 days. The presence of a diffraction band at (002) and (211) was clearly identified.

three to seven days. Further growth after seven days did not seem to improve crystal orientation.

A high-quality cross-sectional TEM specimen of the newly regrown layer was obtained using the FIB technique to assess the robustness of the interface between the repaired layer after 3 days and native enamel. Care was taken to minimize the ion-beam damage to the remineralized layer during the 'lift-out' procedure. The sample was milled to less than 100 nm thickness and attached to the grid to be viewed under TEM. HR-TEM images of this boundary depicted clear lattice fringes from the (300) and (211) planes of the native enamel crystal with distance between the crystal planes (d) being 0.28 nm and 0.29 nm, respectively, while the synthetic crystal at the (002) plane had $d = 0.33$ nm (Fig. 5). The selected area electron diffraction (SAED) plane of the reconstructed layer showed an arc-shaped pattern which suggested a preferred c-axial orientation of the regrown crystals that had a robust chemical attachment to the natural enamel (inset in Fig. 5).

B. The mechanism of chitosan-LRAP in promoting regrowth of enamel-like crystals

Chitosan is a product obtained by the alkaline deacetylation of chitin, a naturally occurring biopolymer derived from the exoskeleton of crustaceans, mollusks, insects, and certain fungi.[30] Chitosan is utilized in the field of regenerative medicine and material research due to its versatile biological properties, which allowed us here to explore its role as an efficient scaffold that could act as a template for crystal growth while presenting amelogenin proteins and peptides. It is of commercial interest due to its biodegradability, biocompatibility, nontoxicity, antimicrobial activity and adhesive properties.[31] A comparison was drawn between the regrown biomimetic layer formed by chitosan only, chitosan–LRAP, and chitosan–rP172 (full-length amelogenin) hydrogels at the end of 3 days of remineralization.

https://doi.org/10.1557/jmr.2016.64 Published online by Cambridge University Press

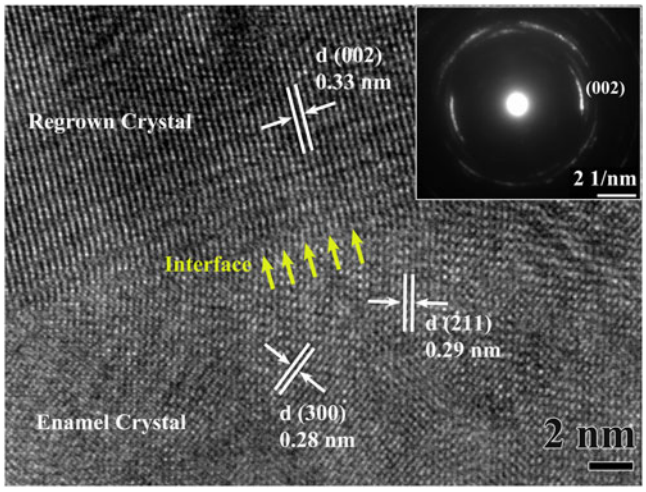


FIG. 5. HR-TEM image of the boundary between enamel and the newly grown crystal showing a robust interface at nanoscale level (represented by yellow arrows). (Inset) The SAED image of the regrown layer.

Smaller, scattered crystallites were observed in patches over the demineralized enamel window in the chitosan-only group (seen in SEM) whereas in the presence of LRAP–CS, larger and denser organized crystals were seen similar in morphology to the crystals grown under the influence of full-length amelogenin chitosan hydrogel.

Previously, LRAP assemblies have been observed as monomer/dimer-like structures on self-assembled monolayer interfaces[22] similar to what has been seen with recombinant full-length amelogenin (rp(H)M180, rM180, rP172).[32–34] More recently, LRAP has also been shown to be organized as nanochains at a neutral pH, stabilizing ACP in a manner similar to native phosphorylated porcine amelogenin.[23] Such remarkable similarity of LRAP to the native protein in terms of their manner of self-assembly has prompted the use of LRAP as a promising peptide for enamel biomimetic.[24] The smaller size of the peptide also offers the added advantage of reduced cost of production via solid phase peptide synthesis and furthermore may penetrate enamel pores better than its larger counterpart, making the remineralization process more efficient.

We noticed that the rate of crystal growth was much faster in the presence of LRAP in chitosan compared to the control (chitosan only) and to full-length amelogenin (rP172) in chitosan. This may be explained by the hydrophilic nature of LRAP due to the presence of highly charged residues that can actively promote recruitment of Ca^{2+} and PO_4^{3-} ions to the apatite surface. Hence, the strong mineral ion binding capacity of the peptide may actually contribute toward a highly supersaturated environment necessary for mineral nucleation and crystal growth. This would be consistent with previous studies which have suggested a link between the net molecular charge, hydrophilicity of peptides, and acceleration of crystal growth.[35] The role of peptide composition in regulating crystal nucleation and growth has been further elaborated in studies where the more acidic amino acids (e.g., aspartic acid) were shown to reduce the activation free-energy barrier and hasten mineral growth.[36,37] Although the exact mechanism of mineralization using this protein–chitosan hydrogel is yet to be fully elicited, we hypothesize a cluster-growth model wherein conglomeration and phase transition of the mineral prenucleation clusters occur as they transform into organized apatite crystals with time.[13] The contribution of amelogenin in mineralization may be attributed to the stabilization of Ca–P nanoclusters/nanochains,[23] believed to be the building blocks of calcium phosphate, which transform to highly oriented apatitic crystals. The possible benefits of using chitosan as a protective carrier agent to combat early caries may be explained by the presence of its free amino groups that bind the hydrogen ions generated when the pH falls below a critical point (~5.5). This prevents the diffusion of the bound acidic hydrogen ions and protects the enamel surface against enamel demineralization. At normal pH levels in the saliva (6.3–7),[38] chitosan (pK_a 6.5) remains insoluble and interacts weakly with amelogenin. The limited solubility of chitosan at neutral pH affords a unique opportunity to deliver drugs, genes, and peptides.[39] Alternatively, another way of understanding the mineralizing mechanism could be that immersion of hydrogel in a supersaturated calcium phosphate remineralization solution generates nucleation sites for calcification. The presence of a highly charged phosphorylated LRAP may further promote attraction of mineral ions and regulate organized crystal growth within the naturally inert chitosan hydrogel. We used phosphorylated LRAP in our study based on previous studies, which have reported the significance of a single phosphorylation on serine-16. It has been proposed that phosphorylation induces conformational changes,[23,40] both in solution and on the surface, enhancing protein-mineral interactions and stabilizing the ACP phase.[41] Phosphorylation may also alter the LRAP–HAP interface where selective residues move closer to the apatite surface.[42] Hence, the addition of peptide sequences containing acidic residues or functional groups like phosphate may promote interaction with the apatite surface leading to CaP precipitation and this mineralizes the hydrogel in time.[43] The aqueous environment provided by the hydrogel mimics the in vivo gel-like environment during the biomineralization process that is conducive for crystal development while offering a protective environment for the delivery of peptides to target sites.

This peptide chitosan-based gel may provide a promising treatment alternative for the management of early carious lesions. Recently, we reported a reduction in the subsurface carious lesion from ~100 μm to ~50 μm after treatment with AMEL–CS gel in a pH cycle model after 7 days. AMEL–CS could repair artificial incipient caries by regrowing oriented crystals and reducing the depth of the lesions by up to 50–70% under pH-cycling conditions.[44]

https://doi.org/10.1557/jmr.2016.64 Published online by Cambridge University Press

C. Mechanical properties of the regrown biomimetic layer

Figure 6 depicts the hardness of sound enamel, demineralized enamel, chitosan treated enamel, full-length amelogenin-chitosan treated enamel, and LRAP–chitosan treated enamel. ANOVA revealed significant differences among these groups ($P < 0.0001$). Multiple comparisons testing determined that all groups differed from one another ($P < 0.05$), except for the full-length amelogenin and LRAP treated groups ($P > 0.05$). After mineralization in a chitosan hydrogel control, some recovery occurred (~215 HV). However, after treatment with LRAP–CS for only 3 days, the hardness of the demineralized tooth sample increased by almost 52% when compared to the demineralized enamel (~151 to ~291 HV). There was a substantial and significant increase over the chitosan-only control. In a recent study by Shafiei et al., application of LRAP peptide in solution at a concentration of 1 mg/ml, on bovine enamel resulted in hardness recovery of only 28.4%.[24] The LRAP–CS test group did not differ from the full-length amelogenin–CS test group, suggesting that the much smaller LRAP protein retained the functionality of native amelogenin. LRAP–CS was successful in recovering most, ~87%, of the hardness of healthy enamel. This encouraging finding suggests that LRAP–CS strongly enhanced surface hardening of the acid-treated tooth slices, although the contribution of the underlying repaired enamel to the hardness of regrown layer (10 μm thick) cannot be excluded. The hardness of such layers can be improved by future application of enzymes or proteinases in the regrowth experiment to remove possible occluded organic material in the layer.[45]

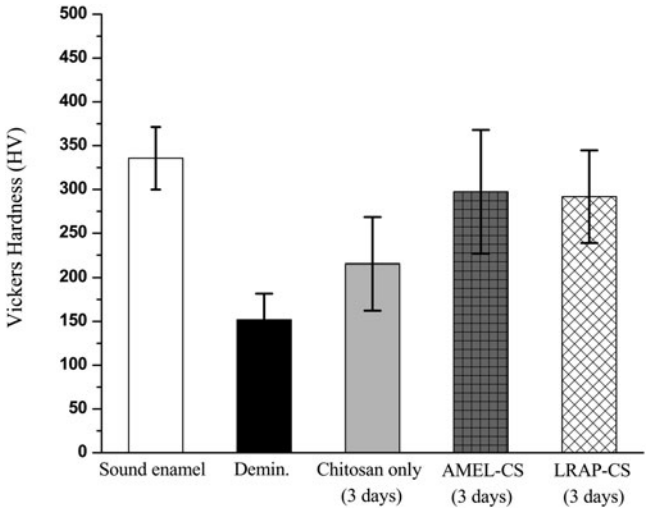


FIG. 6. VMH for healthy enamel, demineralized enamel, and hydrogel treated enamel after 3 days of remineralization cycle using chitosan only, AMEL–CS and LRAP–CS. The error bars represent standard deviation ($n = 3$). Demin: demineralization (7 day). Tukey multiple comparisons revealed that all groups differed from one another ($P < 0.05$), except for the full-length amelogenin and LRAP treated groups ($P > 0.05$).

IV. CONCLUSION

We propose that the chitosan–peptide hydrogel system acts as an organic template on acid-treated enamel surfaces and allows the LRAP peptide to promote faster mineral induction and results in organized crystal growth of hydroxyapatite. It also provides a remarkably robust mineral interface on the enamel surface and increases the surface hardness significantly. This novel technique for replicating enamel-like tissue may have promising prospects for treating incipient caries or white spot lesions. Designing smaller amelogenin-inspired peptides and optimizing the experimental conditions and treatment protocol may enhance the physical properties and durability of the enamel biomimetic layer and should be considered for further studies.

ACKNOWLEDGMENT

This work was supported by NIH-NIDCR grants DE-13414 and DE-020099 to J.M.O. and the USC Coulter Translational Partnership Program. The authors would like to thank Prof. Steven Nutt and Mr. Yuzheng Zhang for assistance with the Focus Ion Beam, the Center for Electron Microscopy and Microanalysis (CEMMA) at USC for electron microscopy and Gabriel Garcia de Carvalho for lab assistance.

REFERENCES

1. H. Chai, J.J.W. Lee, P.J. Constantino, P.W. Lucas, and B.R. Lawn: Remarkable resilience of teeth. *Proc. Natl. Acad. Sci. U. S. A.* **106**, 7289–7293 (2009).
2. J. Moradian-Oldak: Protein-mediated enamel mineralization. *Front. Biosci.* **17**, 1996–2023 (2012).
3. A.R.T. Cate: Tooth enamel—Its composition properties and fundamental structure. *J. Anat.* **100**, 416 (1966).
4. A.G. Fincham, J. Moradian-Oldak, and J.P. Simmer: The structural biology of the developing dental enamel matrix. *J. Struct. Biol.* **126**, 270–299 (1999).
5. J. Moradian-Oldak: Amelogenins: Assembly, processing and control of crystal morphology. *Matrix Biol.* **20**, 293–305 (2001).
6. H. Deyhle, S.N. White, O. Bunk, and F. Beckmann, B. Muller: Nanostructure of carious tooth enamel lesion. *Acta Biomater.* **10**, 355–364 (2014).
7. Q. Ruan and J. Moradian-Oldak: Amelogenin and enamel biomimetics. *J. Mater. Chem. B* **3**, 3112–3129 (2015).
8. J. Kirkham, A. Firth, D. Vernals, N. Boden, C. Robinson, R.C. Shore, S.J. Brookes, and A. Aggeli: Self-assembling peptide scaffolds promote enamel remineralization. *J. Dent. Res.* **86**, 426–430 (2007).
9. S. Mann, J. Fletcher, D. Walsh, and C.E. Fowler: Electrospun mats of PVP/ACP nanofibres for remineralization of enamel tooth surfaces. *CrystEngComm* **13**, 3692–3697 (2011).
10. Y. Fan, X. Xu, J.F. Zhang, J.T. Twomley, Z.T. Wen, S. Liao, T. Lallier, J.L. Hagan, and Z. Sun: Novel amelogenin-releasing hydrogel for remineralization of enamel artificial caries. *J. Bioact. Compat. Polym.* **27**(6), 585–603 (2012).
11. E.C. Reynolds, N.J. Cochrane, S. Saranathan, F. Cai, and K.J. Cross: Enamel subsurface lesion remineralisation with casein phosphopeptide stabilised solutions of calcium, phosphate and fluoride. *Caries Res.* **42**, 88–97 (2008).

https://doi.org/10.1557/jmr.2016.64 Published online by Cambridge University Press

12. K. Yamagishi, K. Onuma, T. Suzuki, F. Okada, J. Tagami, M. Otsuki, and P. Senawangse: Materials chemistry: A synthetic enamel for rapid tooth repair. *Nature* **433**(7028), 819 (2005).
13. Q.C. Ruan, Y.Z. Zhang, X.D. Yang, S. Nutt, and J. Moradian-Oldak: An amelogenin-chitosan matrix promotes assembly of an enamel-like layer with a dense interface. *Acta Biomater.* **9**, 7289–7297 (2013).
14. Q.C. Ruan and J. Moradian-Oldak: Development of amelogenin-chitosan hydrogel for in vitro enamel regrowth with a dense interface. *J. Visualized Exp.* (89), e51606 (2014).
15. S. Habelitz, P.K. DenBesten, S.J. Marshall, G.W. Marshall, and W. Li: Self-assembly and effect on crystal growth of the leucine-rich amelogenin peptide. *Eur. J. Oral Sci.* **114**, 315–319 (2006).
16. B.J. Tarasevich, U. Perez-Salas, D.L. Masica, J. Philo, P. Kienzle, S. Krueger, C.F. Majkrzak, J.L. Gray, and W.J. Shaw: Neutron reflectometry studies of the adsorbed structure of the amelogenin, LRAP. *J. Phys. Chem. B* **117**, 3098–3109 (2013).
17. W.J. Shaw, K. Ferris, B. Tarasevich, and J.L. Larson: The structure and orientation of the C-terminus of LRAP. *Biophys. J.* **94**, 3247–3257 (2008).
18. L. Addadi, J. Moradianoldak, H. Furedimilhofer, S. Weiner, and A. Veis: Stereochemical aspects of crystal regulation in calcium phosphate-associated mineralized tissues. *Int. Congr. Ser.* **1002**, 153–162 (1992).
19. L. Addadi and S. Weiner: Interactions between acidic proteins and crystals—Stereochemical requirements in biomineralization. *Proc. Natl. Acad. Sci. U. S. A.* **82**, 4110–4114 (1985).
20. D.B. DeOliveira and R.A. Laursen: Control of calcite crystal morphology by a peptide designed to bind to a specific surface. *J. Am. Chem. Soc.* **119**, 10627–10631 (1997).
21. B.J. Tarasevich, J.S. Philo, N.K. Maluf, S. Krueger, G.W. Buchko, G.Y. Lin, and W.J. Shaw: The leucine-rich amelogenin protein (LRAP) is primarily monomeric and unstructured in physiological solution. *J. Struct. Biol.* **190**, 81–91 (2015).
22. B.J. Tarasevich, S. Lea, and W.J. Shaw: The leucine rich amelogenin protein (LRAP) adsorbs as monomers or dimers onto surfaces. *J. Struct. Biol.* **169**, 266–276 (2010).
23. E. Le Norcy, S.Y. Kwak, F.B. Wiedemann-Bidlack, E. Beniash, Y. Yamakoshi, J.P. Simmer, and H.C. Margolis: Leucine-rich amelogenin peptides regulate mineralization in vitro. *J. Dent. Res.* **90**, 1091–1097 (2011).
24. F. Shafiei, B.G. Hossein, M.M. Farajollahi, M. Fathollah, B. Marjan, and J.K. Tahereh: Leucine-rich amelogenin peptide (LRAP) as a surface primer for biomimetic remineralization of superficial enamel defects: An in vitro study. *Scanning* **37**, 179–185 (2015).
25. F. Boabaid, C.W. Gibson, M.A. Kuehl, J.E. Berry, M.L. Snead, F.H. Nociti, E. Katchburian, and M.J. Somerman: Leucine-rich amelogenin peptide: A candidate signaling molecule during cementogenesis. *J. Periodontol.* **75**, 1126–1136 (2004).
26. R. Warotayanont, D.H. Zhu, M.L. Snead, and Y. Zhou: Leucine-rich amelogenin peptide induces osteogenesis in mouse embryonic stem cells. *Biochem. Biophys. Res. Commun.* **367**, 1–6 (2008).
27. C. Robinson, R.C. Shore, S.J. Brookes, S. Strafford, S.R. Wood, and J. Kirkham: The chemistry of enamel caries. *Crit. Rev. Oral Biol. Med.* **11**, 481–495 (2000).
28. S. Busch, U. Schwarz, and R. Kniep: Chemical and structural investigations of biomimetically grown fluorapatite–gelatin composite aggregates. *Adv. Funct. Mater.* **13**, 189–198 (2003).
29. O. Prymak, V. Sokolova, T. Peitsch, and M. Epple: The crystallization of fluoroapatite dumbbells from supersaturated aqueous solution. *Cryst. Growth Des.* **6**, 498–506 (2006).
30. F.A. Al Sagheer, M.A. Al-Sughayer, S. Muslim, and M.Z. Elsabee: Extraction and characterization of chitin and chitosan from marine sources in Arabian Gulf. *Carbohydr. Polym.* **77**, 410–419 (2009).
31. A. Lagarto, N. Merino, O. Valdes, J. Dominguez, E. Spencer, N. de la Paz, and G. Aparicio: Safety evaluation of chitosan and chitosan acid salts from Panurilus argus lobster. *Int. J. Biol. Macromol.* **72**, 1343–1350 (2015).
32. B.J. Tarasevich, S. Lea, W. Bernt, M. Engelhard, and W.J. Shaw: Adsorption of amelogenin onto self-assembled and fluoroapatite surfaces. *J. Phys. Chem. B* **113**, 1833–1842 (2009).
33. B.J. Tarasevich, S. Lea, W. Bernt, M.H. Engelhard, and W.J. Shaw: Rapid communication changes in the quaternary structure of amelogenin when adsorbed onto surfaces. *Biopolymers* **91**, 103–107 (2009).
34. C.L. Chen, K.M. Bromley, J. Moradian-Oldak, and J.J. DeYoreo: In situ AFM study of amelogenin assembly and disassembly dynamics on charged surfaces provides insights on matrix protein self-assembly. *J. Am. Chem. Soc.* **133**, 17406–17413 (2011).
35. S. Elhadj, J.J. De Yoreo, J.R. Hoyer, and P.M. Dove: Role of molecular charge and hydrophilicity in regulating the kinetics of crystal growth. *Proc. Natl. Acad. Sci. U. S. A.* **103**, 19237–19242 (2006).
36. S. Piana, F. Jones, Z. Taylor, P. Raiteri, and J.D. Gale: Exploring the role of ions and amino acids in directing the growth of minerals from solution. *Mineral. Mag.* **72**, 273–276 (2008).
37. X.D. Yang, B.Q. Xie, L.J. Wang, Y.L. Qin, Z.J. Henneman, and G.H. Nancollas: Influence of magnesium ions and amino acids on the nucleation and growth of hydroxyapatite. *CrystEngComm* **13**, 1153–1158 (2011).
38. K. Bowman and K.W. Leong: Chitosan nanoparticles for oral drug and gene delivery. *Int. J. Nanomed.* **1**(2), 117–128 (2006).
39. R.M. Stephan: pH and dental caries. *J. Dent. Res.* **26**, 340 (1947).
40. D.L. Masica, J.J. Gray, and W.J. Shaw: Partial high-resolution structure of phosphorylated and non-phosphorylated leucine-rich amelogenin protein adsorbed to hydroxyapatite. *J. Phys. Chem. C* **115**, 13775−13785 (2011).
41. S-Y. Kwak, R.B. Wiedemann-Bidlack, E. Beniash, Y. Yamakoshi, J.P. Simmer, A. Litman, and H.C. Margolis: Role of 20-kDa amelogenin (P148) phosphorylation in calcium phosphate formation in vitro. *J. Biol. Chem.* **284**, 18972−18979 (2009).
42. J-X. Lu, S.Y. Xu, and W.J. Shaw: Phosphorylation and ionic strength alter the LRAP–HAP interface in the N-terminus. *Biochemistry* **52**, 2196−2205 (2013).
43. K. Gkioni, S.C.G. Leeuwenburgh, T.E.L. Douglas, A.G. Mikos, and J.A. Jansen: Mineralization of hydrogels for bone regeneration. *Tissue Eng.* **16**, 577–585 (2010).
44. Q. Ruan, D. Liberman, R. Bapat', K.C. Balakrishna, J-H. Phark, and J. Moradian-Oldak: Efficacy of amelogenin-chitosan hydrogel in biomimetic repair of human enamel in pH-cycling systems. *J. Biomed. Eng. Health Inform* **2**(1), 123–124 (2016).
45. S. Prajapati, J. Tao, Q. Ruan, J.J. De Yoreo, and J. Moradian-oldak: Matrix Metalloproteinase-20 mediates dental enamel biomineralization by preventing protein occlusion inside apatite crystals. *Biomaterials* **75**, 260–270 (2016).

Supplementary Material

To view supplementary material for this article, please visit http://dx.doi.org/10.1557/jmr.2016.64.

https://doi.org/10.1557/jmr.2016.64 Published online by Cambridge University Press